



Thermodynamic and Exergo-economic Analyses of Waste Heat Recovery of a Two-shaft Turbofan Engine Using Supercritical Carbon Dioxide Brayton Cycle

A. Kamani, I. Mirzaee*, N. Pourmahmoud

Department of Mechanical Engineering, Engineering Faculty, Urmia University, Urmia, Iran

PAPER INFO

Paper history:

Received 20 December 2022

Accepted in revised form 31 January 2023

Keywords:

Energy analysis

Exergy analysis

Exergo-economic analysis

Supercritical carbon dioxide cycle

Turbofan engine

ABSTRACT

In this study, first-law, second-law, and exergo-economic investigations are accomplished to recover the waste heat of a two-shaft turbofan engine applying a supercritical carbon dioxide Brayton cycle. The efficacy of different operating parameters including the inlet temperature of the turbine, the pressure ratio of the compressor, and Mach number on the performance of the proposed system in terms of energy and exergy performance, exergy destruction rate, and annual levelized cost of investment have been examined. The results indicate that the energy performance of the cycle is specified as 42.94%, the second-law performance of the cycle is calculated as 85.88% and the whole power generation amount of the system is achieved to be 9806 kW. Also, the results display that among the various components of the proposed system, the maximum amount of exergy destruction occurred in the low-pressure compressor, the fan, and the mixer. It is found that by increasing the inlet temperature of the high-pressure turbine, the first-law efficiency and the second-law efficiency of the proposed cycle decrease while the total cost rate and exergy destruction rate increase. Moreover, it is inferred that the thermodynamic efficiency of the system rises when the pressure ratio of the compressor and Mach number increase. The outcomes also demonstrate that concerning the capital costs and exergy destruction costs of components, the highest amount is obtained for high-pressure turbine and recuperator, which are 326.3 \$/h and 358.4 \$/h, respectively.

doi: 10.5829/ijee.2023.14.02.10

NOMENCLATURE

AF	The proportion of the total airflow via the turbofan to the fuel stream	e	Output
c	Exergy unit cost (\$/GJ)	D	Destroyed
\dot{C}	Exergy streams' cost rate (\$/s)	f	Fuel
$\dot{E}x$	The rate of exergy (kW)	fan	Fan
f	Fraction of flow	LPC	Low-pressure compressor
h	Specific enthalpy (kJ kg ⁻¹ K ⁻¹)	LPT	Low-pressure turbine
HC	The heat of combustion of fuel (MJ kg ⁻¹)	$heater$	Heater
K_p	Coefficient of pressure recovery	hs	Heat sink
M	Flight Mach number	HPC	High-pressure compressor
\dot{m}	Mass flow rate (kg s ⁻¹)	HPT	High-pressure turbine
P	Pressure (kPa)	i	input
PR	Pressure ratio	ic	Intercooler
\dot{Q}	The rate of heat transfer (kW)	ph	Physical
SPC	Specific fuel consumption	$prec$	Precompressor
r_k	Relative cost difference	$prop$	Propulsive

*Corresponding Author Email: i.mirzaee@urmia.ac.ir (I. Mirzaee)

s	Specific entropy (kJ/kmol-K)	rec	Recompressor
T	Temperature (K)	$recu$	Recuperator
V	Speed (m s ⁻¹)	$reheater$	Reheater
\dot{W}	Power (kW)	$thrust$	Thrust
Z	Investment cost (\$)	th	Thermal
Subscripts		Greek Symbols	
0	Reference state	η	Efficiency
CC	Combustion chamber	ν	Specific volume

INTRODUCTION

In recent years, issues such as increasing energy costs in the world, preserving the environment with less per capita energy consumption, producing less environmental pollutants, and also obtaining the most useful work from a certain amount of fuel have caused the owners of industries, to carry out extensive investigations to increase productivity and optimizing the system [1-2]. Most of the studies that have been done by the researchers were on power plant cycles, and air cycles such as turbojet or turbofan engines or other derivatives of air engines have received less attention [3].

Due to the wide use of all types of air engines in the world, their thermodynamic analysis is important for improvement. The development of these types of engines based on their different needs and applications, the design of more efficient engines, and also the optimization of the existing engines all benefit from thermodynamic analysis methods [4]. From fossil fuel utilization systems in the world, the share of airplanes is about 3% which means airplanes are responsible for almost 2 % of the GHG emission. The amount of use of air transportation increases year by year which can increase the GHG emission in the future. Therefore, it is crucial to modify the technology and useful efficiency to decrease the environmental impacts caused by aviation [5, 6]. Dinc and Gharbia [7] studied turboprop engine efficiency under different flight speeds and altitudes from an exergy standpoint. The outcomes displayed that the exergy performance obtained was in the range of 23-33 % while the energy efficiency was in the limit of 25-35 %. The authors stated that for higher speeds and altitudes, the exergy efficiency is higher while it is lower for lower speeds and altitudes. Aygun et al. [8] inquired about the function of a variable system engine for eight flight phases compared with the regular martial turbofan. According to the results, the range of varying exergy performance of VCE is achieved betwixt 7.45% and 31.39% while it is between 6.31 and 21.5 % for the CMT engine. Moreover, the index of sustainability of exergy was between 0.31 and 0.34 for the CMT engine and 0.45 and 0.6 for the VCE. Akdeniz et al. [9] executed a 7E inquiry into aero engines applied in military aviation. The conclusions depicted that the first-law and second-law

efficiencies of the overall system were obtained to be 18.25% and 19.37%, respectively. From an exergo-economic standpoint, the whole system's product unit exergy cost rate was evaluated as 98.441 US\$/GJ while the cost rate of exergy was 980.111 US\$/h. In a separate study, Nasir et al. [10] examined the efficiency of an ORC cycle with a superheater combined with a turbofan engine to recuperate the heat losses of the engine. After analyzing the proposed cycle, it is found that by adding an Organic Rankine Cycle (ORC) to the turbofan engine, lower fuel consumption was observed in the engine. Moreover, it is stated that adding a regenerator eventuated in an advance in the system output and thrust power. In another research by Turgut et al. [11], they analyzed and studied a turbofan engine from the exergy viewpoint. The turbofan engine investigated was CF6-type 80 and its exergy analysis was carried out at sea level. Their outcomes revealed that the variations in the exergy efficiency of the engine depend on the variations in the isentropic efficiency of its rotating parts such as the turbine and compressor. Kahraman et al. [12] analyzed the combustor combustion specifications of a small turbojet engine supplied by jet-A fuel and hydrogen. According to the results, hydrogen ignition is superior in terms of the pressure drop and exit temperature plus CO₂ and unburned HC discharges. For a turboshaft engine, Zare et al. [13] accomplished an exergy and exergo-economic investigation of the application of three standard kinds of jet fuels containing JP-4, JP-5, and JP-8. After a parametric study, it is stated that using JP-4 fuel provides higher performance in terms of power unit cost and exergy efficiency. In comparison with other proposed fuels, JP-4 presented 9% and 6 % higher exergy efficiency compared with JP-5 and JP-8, respectively. Farahani et al. [14] carried out the energy and exergy simulation of the TF30-P414 turbofan engine. The impacts of changing some essential factors on the efficiency of the cycle were studied. Among different components of the engine, it is found that the maximum and minimum amount of exergy destruction rates is acquired for the combustion chamber and nozzle, respectively. The outcomes of optimization indicated that the maximum exergy efficiency can be achieved for a flight altitude of 10000 to 15000 meters and Mach number 1.2 to 2.2. Balli et al. [15] investigated a jet

engine J69-T25A from an energy, exergy, and exergoeconomic standpoint. They indicated that the exergetic performance of the AJE is 34.84 %. Moreover, the maximum amount of exergy destruction happens in the combustion chamber. The unit exergy cost and exergy cost of the engine were computed to be 70.956 US\$/GW and 618.643 US\$/ h, respectively. In another study, Coban et al. [16] executed an exergetic and exergoeconomic investigation of a turbojet engine. The outcomes indicated that the highest exergy performance of the components is 99 % for a high-pressure turbine compared with the application of biofuel which is 98.44 % for the case supplied with regular jet fuel. 3E analysis including exergy, exergoeconomic, and environmental investigation of the aircraft engine turbofan (ATFE) in the aerospace industry was studied by Balli and Karakoc [17]. The results indicated that exergy efficiency was calculated to be 20.32%. Moreover, they found that to rise the engine exergy efficiency increased by about 0.26% and the sustainability index decreased by about 0.735% when biofuel was used instead of jet fuel. Finally, it was found that the fuel cost of biofuel is greater than jet fuel.

The literature review indicates that the prior investigations for turboshaft engines mostly concentrate on energy and exergy studies. Moreover, to the best knowledge of the authors, mostly one-shaft turbofan has been studied and any research on two-shaft inquiry and integration of supercritical CO₂ cycle to these types of engines has not been investigated before. Furthermore, in most of the studies, simple configurations of CO₂ have been used. Therefore, the significant purpose of the present study is to exploit an energetic, exergetic, and economic (3E) survey of a hybrid system containing a sustainable efficiency factor, exergetic sustainability index, and exergy efficiency the waste exergy should decrease. Sabzehali et al. [18] studied the effects of different parameters on the GENX 1B70 engine in take-off and on design states. According to the results, the thermal performance and entropy generation rate of the studied engine are increased when the inlet air temperature is reduced and JP10 fuel is applied. Alibeigi et al. [19] energy and environmental investigation of a turboshaft engine studied by adding inlet air cooling and regenerative cooling. They comprehensively studied the effects of different parameters on the performance of the proposed system. Furthermore, they developed a model based on a deep neural network (DNN) to predict the energy-environment efficiency of the system. The reliability of the biofuel dappling in a J69 military turbojet aero engine of Cessna T-37B/C pilot trainer aircraft was studied by Balli et al. [20] in terms of energy, exergy, sustainability, exergoenvironment, and thermoeconomic. supercritical carbon dioxide Brayton cycle with reheating, intercooling, and regeneration to recover the

waste heat of a two-shaft turbofan engine. The main steps for doing this study are:

- Calculation of different parameters for referenced operating conditions
- Performing energy and exergy analysis and obtaining operational parameters for system components
- Developing cost balance formulas and complementary equations
- Computing exergy flow costs and uniting exergy costs of different parts by solving cost balance

SYSTEM DESCRIPTION AND ASSUMPTIONS

Figure 1 depicts the schematic of the system that has been studied and analyzed in this research. The proposed system is a two-shaft turbofan engine that includes a diffuser, a combustion chamber, LP and HP compressors, LP and HP turbines, and a nozzle. In this engine, the air is first drawn into the engine, passes through the diffuser, and then enters a fan. The fan is joined to a low-pressure shaft and it can produce a large amount of air. The hot air exiting the fan is separated into two flows-bypass flow and core flow. The core flow enters the LP and HP compressors, respectively, and the temperature and pressure of the flow rise. The high-pressure air getting into the combustion chamber reacts with the injected fuel and leaves the chamber towards the high and low-pressure turbines with a higher temperature. The HP turbine enables the power needed by the HP compressor and the LP turbine enables the power needed by the fan and LP compressor. The core flow passes through the heater and reheater and is mixed with the bypass flow and then the united stream comes out of the nozzle and the driving force of the engine is produced. To recuperate the heat loss of the hot air exiting the low-pressure turbine of the turbofan engine, a supercritical carbon dioxide Brayton cycle with reheating, intercooling, and regeneration are used. The cycle is combined with a heat exchanger, turbine, recuperator, heat sink, intercooler, and compressor. A low-temperature CO₂ gets into a precompressor and is compressed. The temperature of the working fluid entering the recompressor is decreased in the intercooling. CO₂ gains heat from the higher-temperature fluid, which flows from the LP turbine within the regenerator. Afterward, the heater rises the temperature by the flow leaves the LP turbine of the turbofan engine, to enter the HP turbine. To increment the output of the cycle, a reheater is used which leads to an enhancement in the turbine outlet temperature. After reheating, working fluid gets into the LP turbine to generate power in the generator. The exiting flow has a

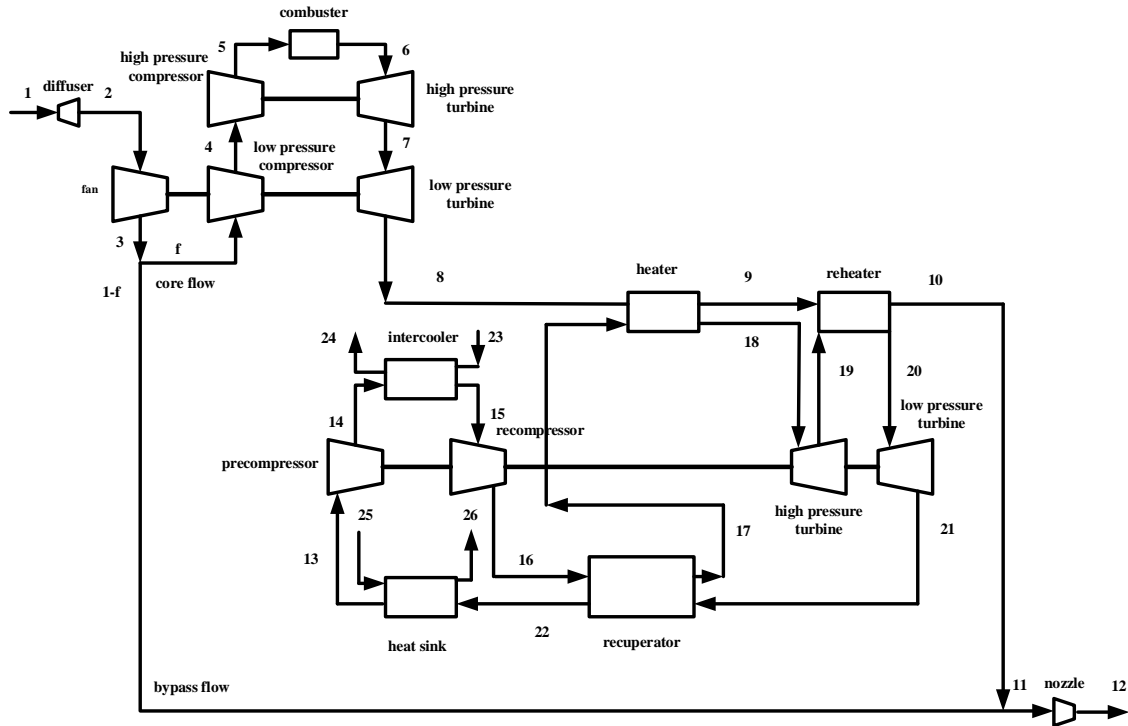


Figure 1. Schematic view of the considered two-shaft turbofan engine

high potential which is transferred to the main compressor exit stream by leaving through a recuperator.

The following general presumptions are considered in the present study [21, 22]:

- The proposed systems are operating in steady-state conditions.
- Variations in kinetic and potential energies and exergies are overlooked.
- The pressure losses of the system components are neglected.
- The incoming engine air contains 79% nitrogen and 21% oxygen.
- The combustion gas mixture as well as air are presumed to be as ideal gases.
- The combustion process is supposed to happen completely.
- The velocity in different sections of the engine is considered zero, except for the inlet section and the outlet section.
- Isentropic efficiencies of the turbomachinery are considered.

MODELING AND ANALYSIS

Thermodynamic analysis

For efficiency simulation of the considered two-shaft turbofan engine, Engineering Equation Solver (EES)

software [23] is applied to model the system. The first law of thermodynamics as well as mass conservation is used to perform the energy analysis. Exergy analysis is another technique to measure the function of systems related to energy. The mass conservation, energy, and exergy balance formulas for a control volume, operating in a steady state process, are represented as follows [24, 25]:

$$\sum_i \dot{m}_i = \sum_e \dot{m}_e \quad (1)$$

$$\sum_i \dot{m}_i h_i + \dot{Q} = \sum_e \dot{m}_e h_e + \dot{W} \quad (2)$$

$$\sum \left(1 - \frac{T_0}{T_k}\right) \dot{Q}_k - \dot{W} + \sum \dot{E}x_{in} - \sum \dot{E}x_{out} - \dot{E}x_D = 0 \quad (3)$$

the total exergy for a flow of matter through a system can be expressed as follows:

$$\dot{E}x = \dot{m}(ex_{kn} + ex_{pt} + ex_{ph} + ex_{ch}) \quad (4)$$

where the terms ex_{kn} , ex_{pt} , ex_{ph} and ex_{ch} represent the kinetic exergy, potential exergy, physical exergy, and chemical exergy, respectively.

The specific physical exergy can be determined as follows [26]:

$$\dot{E}x_{ph} = \dot{m}[(h - h_0) - T_0(s - s_0)] \quad (5)$$

The specific chemical exergy ($C_xH_yO_zS_\sigma$) for the liquid fuels based on the unit mass can be written as follows [27]:

$$\frac{e_{ch,f}}{LHV} = \gamma_f \cong 1.0401 + 0.01728 \frac{y}{x} + 0.0432 \frac{z}{x} + 0.2196 \frac{\sigma}{x} \left(1 - 2.0628 \frac{y}{x}\right) \quad (6)$$

where γ_f denotes the fuel exergy grade function for liquefied fuels and it is calculated to be 1.0616 [9].

The governing equations of the different parts of the turbofan engine are expressed as follows [28]. The entering air velocity into the turbofan engine is obtained from:

$$\tilde{V}_1 = M c_1 \quad (7)$$

The coefficient of pressure recovery for the diffuser is applied to specify the pressure at the diffuser outlet:

$$P_2 = P_1 + K_p \frac{\tilde{V}_1^2}{2v_1} \quad (8)$$

The pressure at the exit point of the fan is provided by:

$$P_3 = (PR)_{fan} P_2 \quad (9)$$

The pressure at the outlet of the LP compressor is calculated by:

$$P_4 = (PR)_{LPC} P_3 \quad (10)$$

Equations 9 and 10 can also be used for the HP compressor. The following equation can be presented for the combustion chamber:

$$f h_5 + \frac{HC}{AF} = \left(f + \frac{1}{AF}\right) h_6 \quad (11)$$

where HC is the fuel heat of combustion and AF is the air-fuel ratio and is described as the proportion of the total airflow through the turbofan to the fuel flow.

The thrust generated by the engine can be obtained by:

$$F_{thrust} = \dot{m} \left[\left(1 + \frac{1}{AF}\right) \tilde{V}_{12} - \tilde{V}_1 \right] \quad (12)$$

The specific fuel consumption is calculated by [29]:

$$SFC = \frac{\dot{m}}{F_{thrust}} \quad (13)$$

The thermal and propulsive performance of the engine is calculated according to following expressions:

$$\eta_{th} = \frac{(\dot{m} + \dot{m}_f) \tilde{V}_{12}^2 - \dot{m} \tilde{V}_1^2}{2 \dot{m}_f HC} \quad (14)$$

$$\eta_{prop} = \frac{2 \tilde{V}_1 F_{thrust}}{(\dot{m} + \dot{m}_f) \tilde{V}_{12}^2 - \dot{m} \tilde{V}_1^2} \quad (15)$$

The equations applied in the thermodynamic analysis of the combined turbofan engine S-CO₂ system components are given in Table 1.

Exergo-economic analysis

The principal target of performing an exergo-economic investigation is to determine the procedure of cost formatting by computing the product unit exergy cost flows in a defined system [33]. By operating an exergo-economic investigation, the researcher receives cost-effective beneficial data that is not available by ordinary economic or exergy estimation. In an exergo-economic survey, to specify the cost rate of each exergy flow, cost balance relations plus appropriate auxiliary equations are applied for each part of the system. The total cost balance equations for a system component can be presented as follows [34-35]:

$$\sum \dot{C}_{out,k} + \dot{C}_{w,k} = \sum \dot{C}_{in,k} + \dot{C}_{q,k} + \dot{Z}_k \quad (16)$$

$$\dot{C}_i = c_i \dot{E}x \quad (17)$$

which $\dot{E}x$ is the exergy rate and C is described as the exergetic unit cost of the flow.

Annual levelized cost of investment can be obtained by [36]:

$$\dot{Z}_k = \left(\frac{CRF \cdot Z_k \cdot \varphi}{N} \right) \quad (18)$$

in which CRF is defined as the Capital Recovery Factor, φ is the maintenance factor and N is determined as the annual operating hours of the system [37]:

$$CRF = \frac{i_r (1 + i_r)^n}{(1 + i_r)^n - 1} \quad (19)$$

in which i_r is defined as the interest rate and n is the system's useful life.

The average cost per unit exergy of fuel is computed by:

$$c_{F,k} = \frac{\dot{C}_{F,k}}{\dot{E}x_{F,k}} \quad (20)$$

The average cost of product exergy for the component k is:

$$c_{P,k} = \frac{\dot{C}_{P,k}}{\dot{E}x_{P,k}} \quad (21)$$

The cost flow rate for the part k generated by the exergy destruction can be described as follows:

$$\dot{C}_{D,k} = c_{F,k} \dot{E}x_{D,k} \quad (22)$$

The exergoeconomic factor for the part k of the system is calculated by:

$$f_k = \frac{\dot{Z}_k}{\dot{Z}_k + \dot{C}_{D,k}} \quad (23)$$

The relative cost difference of the component K is obtained by:

$$r_k = \frac{(c_{P,k} - c_{F,k})}{c_{F,k}} \quad (24)$$

Table 2 presents the cost balances in addition to auxiliary equations for the different components of the two-shaft turbofan engine.

RESULTS AND DISCUSSION

In this part of the study, the results of the energy, exergy, and exergo-economic investigation of a two-shaft turbofan engine are presented. The problem-solving algorithm including inputs, outputs, and the calculation process is shown in Figure 2. This analysis has been done according to changes in some main parameters such as the pressure ratio of the compressor, turbine inlet temperature, and Mach number. The basic design

Table 1. First and second law analysis of the proposed combined cycle [30-32]

Components	Energy equations	Exergy equations
Fan	$\dot{W}_{fan} = \dot{m}(h_3 - h_2)$	$\dot{E}x_{D,fan} = \dot{W}_{fan} - (\dot{E}x_3 - \dot{E}x_2)$
LPC	$\dot{W}_{LPC} = \dot{m}f(h_4 - h_3)$	$\dot{E}x_{D,LPC} = \dot{W}_{LPC} - (\dot{E}x_4 - \dot{E}x_3)$
HPC	$\dot{W}_{HPC} = \dot{m}f(h_5 - h_4)$	$\dot{E}x_{D,HPC} = \dot{W}_{HPC} - (\dot{E}x_5 - \dot{E}x_4)$
Combustion chamber	$f h_5 + \frac{HC}{AF} = \left(f + \frac{1}{AF}\right) h_6$	$\dot{E}x_{D,CC} = \dot{E}x_{fuel} - (\dot{E}x_6 - \dot{E}x_5)$
HPT-engine	$\dot{W}_{HPT} = \left(f + \frac{1}{AF}\right) (h_6 - h_7)$	$\dot{E}x_{D,HPT} = (\dot{E}x_6 - \dot{E}x_7) - \dot{W}_{HPT}$
LPT-engine	$\dot{W}_{LPT} = \left(f + \frac{1}{AF}\right) (h_7 - h_8)$	$\dot{E}x_{D,LPT} = (\dot{E}x_7 - \dot{E}x_8) - \dot{W}_{LPT}$
Precompressor	$\dot{W}_{prec} = \dot{m}_{13}(h_{14} - h_{13})$	$\dot{E}x_{D,prec} = \dot{W}_{prec} - (\dot{E}x_{14} - \dot{E}x_{13})$
Recompressor	$\dot{W}_{rec} = \dot{m}_{15}(h_{16} - h_{15})$	$\dot{E}x_{D,rec} = \dot{W}_{rec} - (\dot{E}x_{16} - \dot{E}x_{15})$
Intercooler	$\dot{Q}_{ic} = \dot{m}_{14}(h_{14} - h_{15})$	$\dot{E}x_{D,ic} = (\dot{E}x_{23} - \dot{E}x_{24}) + (\dot{E}x_{14} - \dot{E}x_{15})$
Heater	$\dot{Q}_{heater} = \dot{m}_8(h_8 - h_9)$	$\dot{E}x_{D,heater} = (\dot{E}x_8 - \dot{E}x_9) + (\dot{E}x_{17} - \dot{E}x_{18})$
Reheater	$\dot{Q}_{reheater} = \dot{m}_9(h_9 - h_{10})$	$\dot{E}x_{D,reheater} = (\dot{E}x_9 - \dot{E}x_{10}) + (\dot{E}x_{19} - \dot{E}x_{20})$
HPT-SCO ₂	$\dot{W}_{HPT-SCO2} = \dot{m}_{18}(h_{18} - h_{19})$	$\dot{E}x_{D,HPT-SCO2} = (\dot{E}x_{18} - \dot{E}x_{19}) - \dot{W}_{HPT-SCO2}$
LPT-SCO ₂	$\dot{W}_{LPT-SCO2} = \dot{m}_{20}(h_{20} - h_{21})$	$\dot{E}x_{D,LPT-SCO2} = (\dot{E}x_{20} - \dot{E}x_{21}) - \dot{W}_{LPT-SCO2}$
Recuperator	$\dot{Q}_{recu} = \dot{m}_{16}(h_{17} - h_{16})$	$\dot{E}x_{D,recu} = (\dot{E}x_{16} - \dot{E}x_{17}) + (\dot{E}x_{21} - \dot{E}x_{22})$
Heat sink	$\dot{Q}_{hs} = \dot{m}_{22}(h_{22} - h_{13})$	$\dot{E}x_{D,hs} = (\dot{E}x_{25} - \dot{E}x_{26}) + (\dot{E}x_{22} - \dot{E}x_{13})$

Table 2. The cost functions, cost balances, and auxiliary equations for each component of the system [13,38,39]

Components	Cost relations	Cost balance	Auxiliary equations
Fan	$\left(\frac{71.1\dot{m}_2}{0.92 - eta_{fan}}\right) \left(\frac{P_3}{P_2}\right) \ln\left(\frac{P_3}{P_2}\right)$	$\dot{C}_2 + \dot{C}_{W,fan} + \dot{Z}_{fan} = \dot{C}_2$	$c_{W,fan} = c_{W,HPT}$
LPC	$\left(\frac{71.1\dot{m}_4}{0.92 - eta_{LPC}}\right) \left(\frac{P_4}{P_3}\right) \ln\left(\frac{P_4}{P_3}\right)$	$\dot{C}_3 + \dot{C}_{W,LPC} + \dot{Z}_{LPC} = \dot{C}_4$	$c_{W,LPC} = c_{W,HPT}$
HPC	$\left(\frac{71.1\dot{m}_5}{0.92 - eta_{HPC}}\right) \left(\frac{P_5}{P_4}\right) \ln\left(\frac{P_5}{P_4}\right)$	$\dot{C}_4 + \dot{C}_{W,HPC} + \dot{Z}_{HPC} = \dot{C}_5$	$c_{W,HPC} = c_{W,HPT}$
Combustion chamber	$\left(\frac{46.08\dot{m}_f}{0.995 - \frac{P_6}{P_5}}\right) (1 + \exp(0.018T_6 - 26.4))$	$\dot{C}_5 + \dot{C}_f + \dot{Z}_{CC} = \dot{C}_6$	-

HPT-engine	$\left(\frac{479.34\dot{m}_6}{0.92 - \eta a_{HPT}}\right) \ln\left(\frac{P_6}{P_7}\right) (1 + \exp(0.036T_6 - 54.4))$	$\dot{C}_6 + \dot{Z}_{HPT} = \dot{C}_7 + \dot{C}_{W,HPT}$	$c_6 = c_7$
LPT-engine	$\left(\frac{479.34\dot{m}_7}{0.92 - \eta a_{LPT}}\right) \ln\left(\frac{P_7}{P_8}\right) (1 + \exp(0.036T_7 - 54.4))$	$\dot{C}_7 + \dot{Z}_{LPT} = \dot{C}_8 + \dot{C}_{W,LPT}$	$c_7 = c_8$
Precompressor	$\left(\frac{71.1\dot{m}_{13}}{0.92 - \eta a_{prec}}\right) \left(\frac{P_{14}}{P_{13}}\right) \ln\left(\frac{P_{14}}{P_{13}}\right)$	$\dot{C}_{13} + \dot{C}_{W,prec} + \dot{Z}_{prec} = \dot{C}_{14}$	$c_{W,prec} = c_{W,HPT}$
Recompressor	$\left(\frac{71.1\dot{m}_{15}}{0.92 - \eta a_{rec}}\right) \left(\frac{P_{16}}{P_{15}}\right) \ln\left(\frac{P_{16}}{P_{15}}\right)$	$\dot{C}_{15} + \dot{C}_{W,rec} + \dot{Z}_{rec} = \dot{C}_{16}$	$c_{W,rec} = c_{W,HPT}$
Intercooler	$2143(A_{ic})^{0.514}$	$\dot{C}_{14} + \dot{C}_{23} + \dot{Z}_{ic} = \dot{C}_{15} + \dot{C}_{24}$	$c_{14} = c_{15}, c_{23} = 0$
Heater	$2681(A_{heater})^{0.59}$	$\dot{C}_8 + \dot{C}_{17} + \dot{Z}_{heater} = \dot{C}_{18} + \dot{C}_9$	$c_8 = c_9$
Reheater	$2681(A_{reheater})^{0.59}$	$\dot{C}_9 + \dot{C}_{19} + \dot{Z}_{reheater} = \dot{C}_{20} + \dot{C}_{10}$	$c_9 = c_{10}$
HPT-SCO ₂	$\left(\frac{479.34\dot{m}_{18}}{0.92 - \eta a_{HPT}}\right) \ln\left(\frac{P_{18}}{P_{19}}\right) (1 + \exp(0.036T_{18} - 54.4))$	$\dot{C}_{18} + \dot{Z}_{HPT} = \dot{C}_{19} + \dot{C}_{W,HPT}$	$c_{18} = c_{19}$
LPT-SCO ₂	$\left(\frac{479.34\dot{m}_{20}}{0.92 - \eta a_{LPT}}\right) \ln\left(\frac{P_{20}}{P_{21}}\right) (1 + \exp(0.036T_{20} - 54.4))$	$\dot{C}_{20} + \dot{Z}_{LPT} = \dot{C}_{21} + \dot{C}_{W,LPT}$	$c_{20} = c_{21}$
Recuperator	$2681(A_{rec})^{0.59}$	$\dot{C}_{16} + \dot{C}_{21} + \dot{Z}_{rec} = \dot{C}_{17} + \dot{C}_{22}$	$c_{21} = c_{22}$
Heat sink	$2143(A_{hs})^{0.514}$	$\dot{C}_{22} + \dot{C}_{25} + \dot{Z}_{hs} = \dot{C}_{26} + \dot{C}_{13}$	$c_{22} = c_{13}, c_{25} = 0$

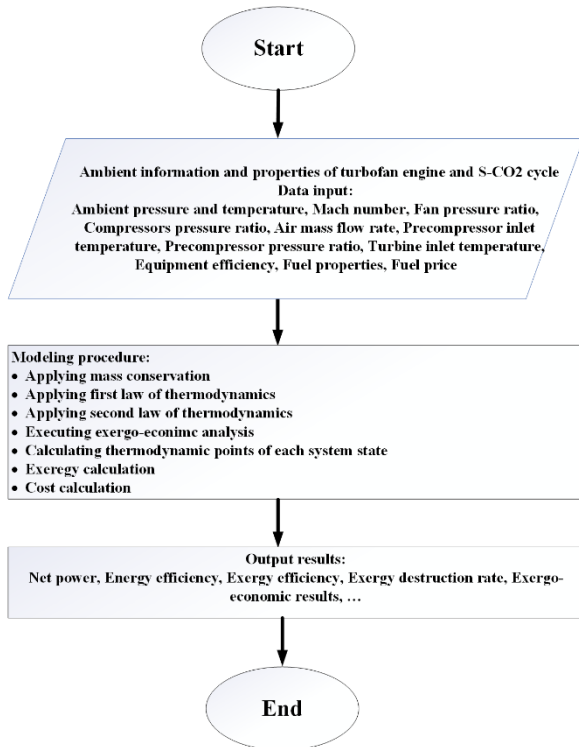


Figure 2. Flowchart of the problem solution

parameters and input data applied in this research are presented in Table 3.

To determine the accuracy of the simulated model, model validation has been carried out. The results of the present model have been compared with the results acquired by Balli et al. [30] and are shown in Table 4. As

it is obvious from the results, between the pressure and temperature of the modeled components with the reference data, the temperature difference is less than 5 K and the pressure difference is less than 5 kPa, which demonstrates a good agreement.

In Table 5, the results for the energy, exergy, and exergoeconomic efficiency of the proposed integrated system are listed. With the initially chosen parameters, the total power generated by the combined system is computed as 9806 kW and the engine and S-CO₂ turbines produced power is 12469 kW and 483.38 kW, respectively. The energy and exergy performance of the proposed system are computed to be 42.94% and 85.88%, respectively. The total levelized cost of system investment is computed to be 436.2 \$/h, the total exergy destruction cost is 19.183 \$/h, and the total exergy destruction rate is achieved at 1101 kW.

Table 6 depicts the results of the exergoeconomic investigation of the proposed combined system. From an exergo-economic perspective, the amount of $\dot{C}_{D,k} + \dot{Z}_k$ shows the significance of the process component. The results indicate that the HP turbine of the turbofan engine has the maximum amount of $\dot{C}_{D,k} + \dot{Z}_k$ which is followed by the recuperator. Therefore, these two units are remarked as the most crucial components. Furthermore, the precompressor, reheater, and intercooler show low values demonstrating that these components are less important compared with other components from the exergo-economic standpoint. Another factor that is an important exergo-economic indicator, is the exergoeconomic factor (f_k). When this indicator is high, it shows that the total cost of the system can be reduced by decreasing the investment cost of the components.

The portion of each part in the whole exergy destruction is displayed in Figure 3. Exergy destruction is a measure to show if the system performs well or not. That means being aware of the source of the exergy destruction and trying to decrease it can help to improve the system's performance. It is inferred that the maximum amount of exergy destruction happens at the low-pressure compressor of the turboshaft engine (31.32%) followed by the fan (30.62%) and the mixer (28.6%). All these three components are parts of the two-shaft turbofan engine cycle. To improve the performance of the overall system, increasing efforts should be made to reduce the exergy destruction in the above-mentioned units.

Figure 4 indicates the variation of the inlet temperature of the high-pressure turbine on the total cost rate. It is perceived that the energy efficiency of the proposed system reduces from 44.34% to 32.9% with the rise in the inlet temperature of the turbine from 1550 to 1800 K while the total cost rate enhances. The enhancement in inlet temperature assists to obtain in the

Table 3. Main assumptions and input parameters assumed in the simulation

Parameter	Symbol	Value
Mach number [40]	M	0.85
Reference temperature [40]	$T_0(K)$	227
Reference pressure	$P_0(kPa)$	101
Isentropic efficiency of the engine turbine [40]	$\eta_{t,engine}(\%)$	90
Isentropic efficiency of the engine compressor [40]	$\eta_{c,engine}(\%)$	89
The pressure ratio of the fan [40]	PR_{fan}	1.6
The pressure ratio of the low-pressure engine compressor [40]	$PR_{LPC,engine}$	2.5
The pressure ratio of the high-pressure engine compressor [40]	$PR_{HPC,engine}$	12
Turbine inlet temperature, Engine [40]	$TIT_{engine}(K)$	1573
Precompressor inlet	$T_{13}[K]$	305.2
Precompressor pressure ratio	PR_{prec}	1.4
Turbine inlet temperature	$TIT(K)$	650.2
The inlet temperature of the water	$T_{water,inlet}[K]$	298.2
The temperature difference of the cooling water	ΔT	10
Precompressor and recompressor isentropic efficiency [40]	$\eta_c(\%)$	0.89
Isentropic efficiency of the turbine [40]	$\eta_t(\%)$	0.9

Table 4. Comparison between the results of the present survey and the results of Balli et al. [30]

Engine component	P (kPa)		T (K)	
	Present study	Ref [30]	Present study	Ref [30]
Compressor inlet	101.325	101.325	288.15	288.15
Compressor outlet	417.86	415.433	475.1	470.5
Combustion chamber	101.325	101.325	298.15	298.15
Turbine inlet	396.12	394.661	1031.65	1028.15
Nozzle inlet	135.318	133.783	891.06	889.9
Nozzle outlet	132.43	131.108	887.89	885.45

Table 5. The energy, exergy, and exergoeconomic results were obtained for the integrated system

Parameter	Value
$\eta_{th}(\%)$	42.94
$\eta_{ex}(\%)$	85.88
$\dot{W}_{net}(kW)$	9806
$\dot{W}_{turb,engine}(kW)$	12469
$\dot{W}_{turb,SCO_2}(kW)$	483.38
$\dot{E}x_{D,tot}(kW)$	1101
$\dot{Z}_{tot}(\$/h)$	436.2
$\dot{C}_{D,tot}(\$/h)$	19.183

Table 6. Exergoeconomic results of the combined system

Component	$\dot{C}_{D,k}$	\dot{Z}_k	$\dot{C}_{D,k} + \dot{Z}_k$	$r_k(\%)$	$f_k(\%)$
Fan	85.21	3.55	88.76	5.76	3.99
LPC	87.63	1.44	89.07	8.96	1.61
HPC	54.27	28.18	82.45	3.78	34.18
Combustion chamber	116.4	2.12	118.52	46.42	1.79
HPT-engine	70.93	326.3	397.23	2.9	82.15
LPT-engine	25.21	5.94	31.15	4	19.08
Precompressor	9.59	0.11	9.7	11.76	1.13
Recompressor	23.3	0.25	23.55	11.65	1.06
Intercooler	4.57	7.35	11.92	85.34	61.66
Heater	114.08	14.45	128.53	29.85	11.24
Reheater	0.69	9.16	9.85	3.79	92.99
HPT-SCO ₂	16.59	0.61	17.2	4.17	3.54
LPT-SCO ₂	51.04	1.69	52.73	5.17	3.21
Recuperator	358.4	25.37	383.77	34.11	6.61
Heat sink	103.8	9.61	113.41	295.6	8.47

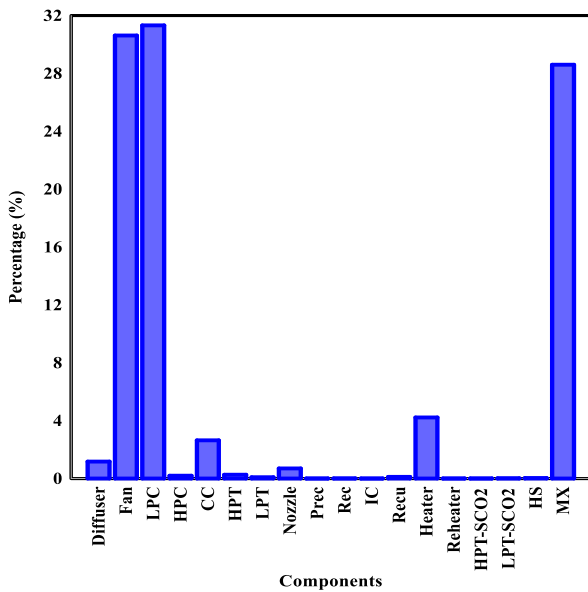


Figure 3. The portion of each part of the system in total exergy destruction

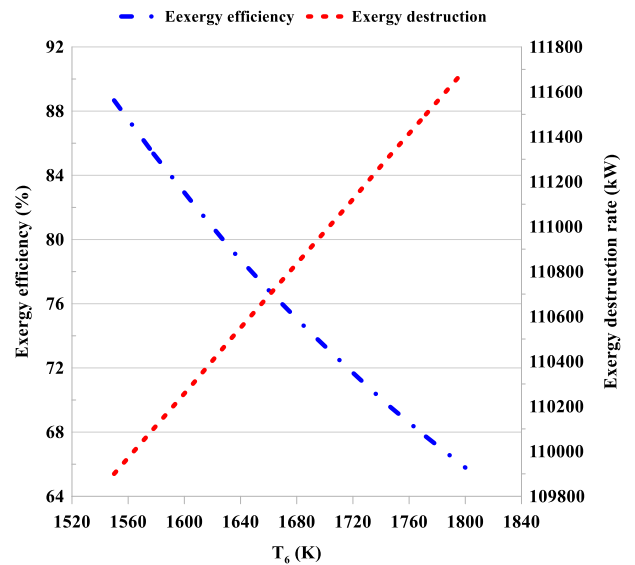


Figure 5. The impact of high-pressure inlet temperature on the exergy destruction rate and exergy performance

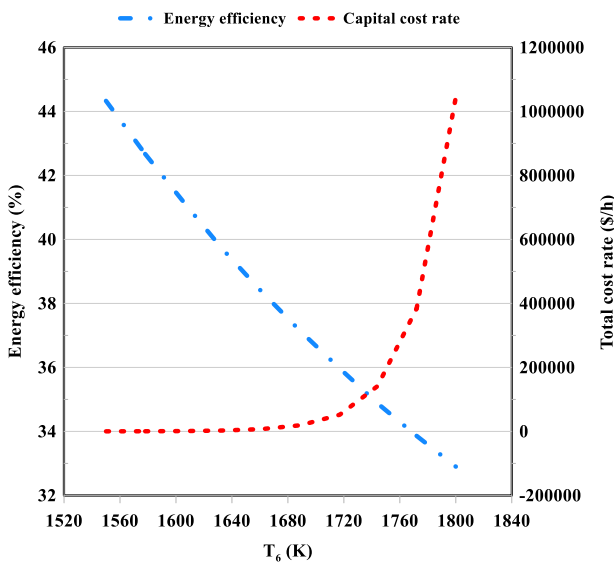


Figure 4. The impact of the inlet temperature of the HP turbine on the total cost rate and energy performance

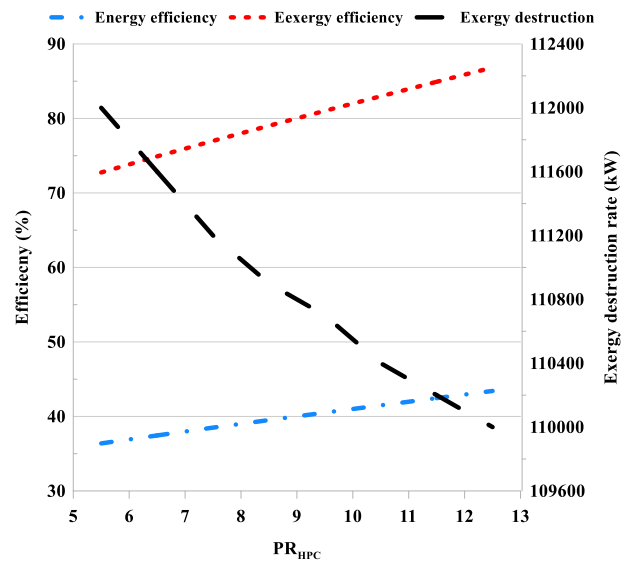


Figure 6. The impact of high-pressure compressor pressure ratio on the efficiencies and exergy destruction rate

net efficiency of the total system as well as a rise in the total heat. The rate of the rise in the total heat of the system surpasses the rate of rise in the total net power; therefore, the energy efficiency of the cycle decreases. On the other hand, it can be inferred that by the increment of turbine inlet temperature, the amount of increase in total cost is not significant but at higher temperatures, a sharp increase was achieved.

Figure 5 depicts the changes in exergy destruction rate and second-law efficiency of the proposed cycle with high-pressure turbine inlet temperature. It is noticed the overall exergetic performance drops linearly from a value

of 88.67% down to 65.79% which is 25.8% lower as the high-pressure inlet temperature increases from 1550 to 1800 K; although the exergy destruction rises 1.6%. The cause for the decrease in the exergy efficiency is that when the inlet temperature goes up, the gap in exergy amounts between the inlet and outlet flows increases. It means that the impact of the entering exergy is more prevailing than the departing exergy.

Figure 6 displays the impact of PR_{HPC} on the energetic and exergetic efficiencies and exergy destruction rate of the proposed system. According to the graphs it can be found that by the growth in the pressure ratio of the

compressor from 5.5 to 12.5, energy and exergy efficiencies increase while a reduction happens in the total exergy destruction rate of the proposed system. When the pressure ratio of the compressor rises, the produced power by the turbine and the used power by the compressors are enhanced too. However, the increment in turbine efficiency is superior to the growth in compressor power consumption as PR_{HPC} goes up which caused an increase in the efficiencies.

The impact of Mach number variation on the exergy and energy efficiency of the system is depicted in Figure 7. The graphs show that when the Ma number of the airplane changed from 0 to 0.9, first-law efficiency increases from 36.38% to 43.83%, and exergy efficiency changed from 72.75% to 87.66%. The reason for this increase is that with the increase in the flight Mach number, the input flow rate to the engine has increased, the amount of fuel consumption has increased, and as a result, the engine power has increased.

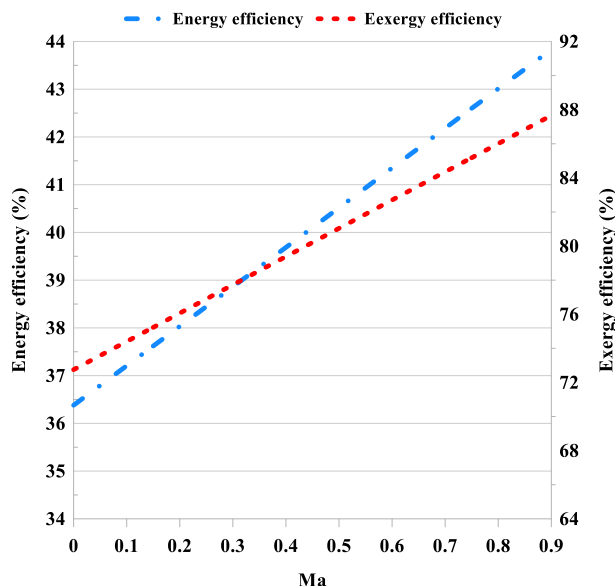


Figure 7. The effect of Ma number variation on the efficiencies of the system

CONCLUSION

In this paper, energy, exergy, and exergoeconomic survey are presented for a two-shaft turbofan engine system combined with a supercritical carbon dioxide cycle. Thermodynamic investigation of the system was carried out by applying energy and exergy methods. The amount of obtained energy and exergy efficiency in addition to the exergy destruction rate of each component and the total system were inquired. Moreover, a parametric survey was accomplished to specify the effect of various factors on the performance of the studied system. The

profits obtained from exergoeconomic analysis are to help recognize the possible states for process betterment by supplying information, and it also supplies a complementary portion in addition to exergy analysis results. The main conclusions of this paper can be listed as follows:

- The first and second law efficiencies of the studied combined system are calculated to be 42.94% and 85.88%, respectively. In addition, the whole power generated by the studied system is achieved to be 9806 kW.
- The highest amount of exergy destruction rate happens within the low-pressure compressor which was about 31% of the whole exergy destruction of the system which is followed by the fan.
- With the increasing inlet temperature of the high-pressure turbine, the energy, and exergy efficiency of the system decrease while an increase can be viewed in the total exergy destruction rate and cost rate of the proposed system.
- An increment in the compressor ratio eventuates in a rise in energy and exergy efficiencies and a reduction in the destruction rate of the integrated system.
- As Mach number increases, the energy and exergy efficiencies of the studied system increase.
- The highest exergy cost rate is for the recuperator which is 358.4 \$/h and the highest levelized cost of investment is for the high-pressure turbine which is 326.3 \$/h.

REFERENCES

1. Habibzadeh, A., Abbasalizadeh, M., Mirzaee, I., Jafarmadar, S. and Shirvani, H., 2023. Thermodynamic Modeling and Analysis of a Solar and Geothermal-driven Multigeneration System Using TiO₂ and SiO₂ Nanoparticles, *Iranian (Iranica) Journal of Energy & Environment*, 14(2), pp.127-138. Doi: 10.5829/ijee.2023.14.02.05
2. Aghagolzadeh Silakhor, R., Jahanian, O. and Alizadeh Kharkehi, B., 2023. Investigating a Combined Cooling, Heating and Power System from Energy and Exergy Point of View with RK-215 ICE Engine as a Prime Mover, *Iranian (Iranica) Journal of Energy & Environment*, 14(1), pp.65-75. Doi: 10.5829/ijee.2023.14.01.09
3. Lee, J.J., 2010. Can we accelerate the improvement of energy efficiency in aircraft systems? *Energy conversion and management*, 51, pp.189-196. Doi: 10.1016/j.enconman.2009.09.011
4. Turgut E., Karakoc H. and Hepbasli A., 2007. Exergy Analysis of a Turbofan Engine: Cf6-80, *University of Anatoly and Ege University, Turkey*.
5. Parker R., 2009. From blue skies to green skies: engine technology to reduce the climate-change impacts of aviation, *Technology Analysis & Strategic Management*, 21, pp.61-78. Doi: 10.1080/09537320802557301
6. Ranasinghe K., Guan K., Gardi A. and Sabatini R., 2019. Review of advanced low-emission technologies for sustainable aviation, *Energy*, 188, pp.115945. Doi: 10.1016/j.energy.2019.115945

7. Dinc A. and Gharbia Y., 2020. Exergy analysis of a turboprop engine at different flight altitude and speeds using novel consideration, *International Journal of Turbo & Jet-Engines*, 39, pp.599-604. Doi: 10.1515/tjeng-2020-0017
8. Aygun, H., Erkara, S. and Turan, O., 2022. Comprehensive exergo-sustainability analysis for a next generation aero engine, *Energy*, 239, pp.122364. Doi: 10.1016/j.energy.2021.122364
9. Akdeniz, H.Y., Balli, O. and Caliskan, H., 2022. Energy, exergy, economic, environmental, energy based economic, exergoeconomic and enviroeconomic (7E) analyses of a jet fuelled turbofan type of aircraft engine, *Fuel*, 322, pp.124165. Doi: 10.1016/j.fuel.2022.124165
10. Nasir, N.A.M., Saadon, S. and Abu Talib, A.R., 2018. Performance analysis of an Organic Rankine Cycle system with superheater utilizing exhaust gas of a turbofan engine, *International Journal of Engineering and Technology*, 7, pp.120-124. Doi: 10.14419/ijet.v7i4.13.21342
11. Turgut, E.T., Karakoc, T.H. and Hepbasli, A., 2007. Exergetic analysis of an aircraft turbofan engine, *International Journal of Energy Research*, 31, pp.1383-1397. Doi: 10.1002/er.1310
12. Kahraman, N., Tangöz, S. and Akansu, S.O., 2018. Numerical analysis of a gas turbine combustor fueled by hydrogen in comparison with jet-A fuel, *Fuel*, 217, pp.66-77. Doi: 10.1016/j.fuel.2017.12.071
13. Zare, V., Khodaparast, S. and Shayan, E., 2021. Comparative thermoeconomic analysis of using different jet fuels in a turboshaft engine for aviation applications, *AUT Journal of Mechanical Engineering*, 5, pp.297-312. Doi: 10.22060/ajme.2020.17888.5877
14. Farahani, S.D., Alibeigi, M. and Sabzehali, M.R., 2021. Energy and Exergy Analysis and Optimization of Turbofan Engine-TF30-P414, *Iranian (Iranica) Journal of Energy & Environment*, 12, pp.307-317. Doi: 10.5829/ijee.2021.12.04.04
15. Balli, O., Aras, H., Aras, N. and Hepbasli, A., 2008. Exergetic and exergoeconomic analysis of an Aircraft Jet Engine (AJE), *International Journal of Exergy*, 5, pp.567-581. Doi: 10.1504/IJEX.2008.020826
16. Coban, K., Şöhret, Y., Colpan, C.O. and Karakoç, T.H., 2017. Exergetic and exergoeconomic assessment of a small-scale turbojet fuelled with biodiesel, *Energy*, 140, pp.1358-1367. Doi: 10.1016/j.energy.2017.05.096
17. Balli, O. and Karakoc, T.H., 2022. Exergetic, exergoeconomic, exergoenvironmental damage cost and impact analyses of an aircraft turbofan engine (ATFE), *Energy*, 256, p.124620. Doi: 10.1016/j.energy.2022.124620
18. Sabzehali, M., Farahani, S.D. and Mosavi, A., 2022. Energy-Exergy Analysis and Optimal Design of a Hydrogen Turbofan Engine, *arXiv preprint arXiv:2208.08890*. Doi: 10.48550/arXiv.2208.08890
19. Alibeigi, M. and Sabzehali, M., 2022. Energy-Environment evaluation and Forecast of a Novel Regenerative turboshaft engine combine cycle with DNN application. *arXiv preprint arXiv:2209.12020*. Doi: 10.48550/arXiv.2209.12020
20. Balli, O., Caliskan, N. and Caliskan, H., 2023. Aviation, energy, exergy, sustainability, exergoenvironmental and thermoeconomic analyses of a turbojet engine fueled with jet fuel and biofuel used on a pilot trainer aircraft, *Energy*, 263, p.126022. Doi: 10.1016/j.energy.2022.126022
21. Coban, K., Colpan, C.O. and Karakoc, T.H., 2017. Application of thermodynamic laws on a military helicopter engine, *Energy*, 140, pp.1427-1436. Doi: 10.1016/j.energy.2017.07.179
22. Akdeniz, H.Y. and Balli, O., 2022. Impact of different fuel usages on thermodynamic performances of a high bypass turbofan engine used in commercial aircraft, *Energy*, 238, p.121745. Doi: 10.1016/j.energy.2021.121745
23. Klein, S.A., 2013. F-Chart Software, Engineering Equation Solver, EES Manual; Chapter 1: Getting Started, Solar Energy Laboratory, University of Wisconsin-Madison: Madison, WI, USA.
24. El-Sayed, A.F., 2017. Aircraft propulsion and gas turbine engines. 2nd edition, CRC press. Doi: 10.1201/9781315156743
25. Cengel, Y.A., Boles, M.A. and Kanoglu, M., 2011. Thermodynamics: an engineering approach (Vol. 5, p. 445). New York: McGraw-hill.
26. Javadi, M.A., Hoseinzadeh, S., Ghasemiasl, R., Heyns, P.S. and Chamkha, A.J., 2020. Sensitivity analysis of combined cycle parameters on exergy, economic, and environmental of a power plant, *Journal of Thermal Analysis and Calorimetry*, 139(1), pp.519-525. Doi: 10.1007/s10973-019-08399-y
27. Rakopoulos, C.D. and Giakoumis, E.G., 2006. Second-law analyses applied to internal combustion engines operation, *Progress in energy and combustion science*, 32(1), pp.2-47. Doi: 10.1016/j.peccs.2005.10.001
28. Farokhi, S., 2014. Aircraft propulsion, *John Wiley & Sons*. ISBN: 9781118806777
29. Balli, O. and Caliskan, H., 2021. On-design and off-design operation performance assessments of an aero turboprop engine used on unmanned aerial vehicles (UAVs) in terms of aviation, thermodynamic, environmental and sustainability perspectives. *Energy Conversion and Management*, 243, p.114403. Doi: 10.1016/j.enconman.2021.114403
30. Sarkar, J. and Bhattacharyya, S., 2009. Optimization of recompression S-CO₂ power cycle with reheating, *Energy Conversion and Management*, 50, pp.1939-1945. Doi: 10.1016/j.enconman.2009.04.015
31. Bejan, A. and Siems, D.L., 2001. The need for exergy analysis and thermodynamic optimization in aircraft development, *Exergy, An International Journal*, 1, pp.14-24. Doi: 10.1016/S1164-0235(01)00005-X
32. Balli, O., Sohret, Y. and Karakoc, H.T., 2018. The effects of hydrogen fuel usage on the exergetic performance of a turbojet engine, *International Journal of Hydrogen Energy*, 43, pp.10848-10858. Doi: 10.1016/j.ijhydene.2017.12.178
33. Bejan, A., Tsatsaronis, G. and Moran, M.J., 1995. Thermal design and optimization, *John Wiley & Sons*. ISBN: 9780471584674
34. Ahmadi, P. and Dincer, I., 2011. Thermodynamic analysis and thermoeconomic optimization of a dual pressure combined cycle power plant with a supplementary firing unit, *Energy Conversion and Management*, 52, pp.2296-2308. Doi: 10.1016/j.enconman.2010.12.023
35. Baghernejad, A. and Yaghoubi, M., 2010. Exergy analysis of an integrated solar combined cycle system, *Renewable Energy*, 35, pp.2157-2164. Doi: 10.1016/j.renene.2010.02.021
36. Valero, A., Lozano, M.A., Serra, L., Tsatsaronis, G., Pisa, J., Frangopoulos, C. and von Spakovsky, M.R., 1994. CGAM problem: definition and conventional solution, *Energy*, 19, pp.279-286. Doi: 10.1016/0360-5442(94)90112-0
37. Javadi, M., Hoseinzadeh, S., Ghasemiasl, R., Heyns, P.S., and Chamkha, A., 2020. Sensitivity analysis of combined cycle parameters on exergy, economic, and environmental of a power plant, *Journal of Thermal Analysis and Calorimetry*, 139, pp.519-525. Doi: 10.1007/s10973-019-08399-y

38. Ma, Y., Morozjuk, T., Liu, M., Yan, J. and Liu, J., 2019. Optimal integration of recompression supercritical CO₂ Brayton cycle with main compression intercooling in solar power tower system based on exergoeconomic approach, *Applied Energy*, 242, pp.1134-1154. Doi: 10.1016/j.apenergy.2019.03.155
39. Sun, L., Wang, D. and Xie, Y., 2021. Energy, exergy and exergoeconomic analysis of two supercritical CO₂ cycles for waste heat recovery of gas turbine, *Applied Thermal Engineering*, 196, pp.117337. Doi: 10.1016/j.applthermaleng.2021.117337
40. Klein, S. and Nellis, G., 2011. *Thermodynamics*. Cambridge University Press.

COPYRIGHTS

©2021 The author(s) This is an open access article distributed under the terms of the Creative Commons Attribution (CC BY 4.0), which permits unrestricted use, distribution, and reproduction in any medium, as long as the original authors and source are cited No permission is required from the authors or the publishers



Persian Abstract

چکیده

در این بررسی، به بررسی قانون اول، قانون دوم و تحلیل انرژی-اقتصادی برای بازیابی گرمای اتلافی یک موتور توربوفن دو شفته با استفاده از یک چرخه دی اکسید کربن فوق بحرانی برایتون پرداخته می‌شود. تاثیر پارامترهای عملیاتی مختلف از جمله دمای ورودی توربین، نسبت فشار کمپرسور و عدد ماخ بر عملکرد سیستم پیشنهادی از نظر عملکرد انرژی و انرژی، نرخ تخریب انرژی و هزینه یکسان شده سالانه سرمایه‌گذاری مورد بررسی قرار گرفت. نتایج حاکی از آن است که عملکرد انرژی چرخه ۴۲/۹۴ درصد، عملکرد قانون دوم چرخه ۸۵/۸۸ درصد و مقدار کل تولید برق سیستم ۹۸۰۶ کیلووات به دست آمده است. همچنین، نتایج نشان می‌دهد که در بین اجزای مختلف سیستم پیشنهادی، بیشترین میزان تخریب انرژی در کمپرسور کم فشار، فن و میکسر رخ داده است. این موضوع مشخص شد که با افزایش دمای ورودی توربین فشار بالا، راندمان قانون اول و دوم سیکل پیشنهادی کاهش می‌یابد در حالی که نرخ کل هزینه و نرخ تخریب انرژی افزایش می‌یابد. علاوه بر این، استنباط می‌شود که با افزایش نسبت فشار کمپرسور و عدد ماخ، بازده ترمودینامیکی سیستم افزایش می‌یابد. نتایج همچنین نشان می‌دهد که با توجه به هزینه‌های سرمایه و هزینه‌های تخریب انرژی قطعات، بیشترین مقدار برای توربین فشار بالا و ریکاپراتور به دست می‌آید که به ترتیب ۳۲۶/۳ دلار در ساعت و ۳۵۸/۴ دلار در ساعت هستند.